

Tropical Pacific–Driven Decadal Energy Transport Variability

WILCO HAZELEGER AND CAMIEL SEVERIJNS

Royal Netherlands Meteorological Institute (KNMI), De Bilt, Netherlands

RICHARD SEAGER

Lamont-Doherty Earth Observatory, Columbia University, Palisades, New York

FRANCO MOLTENI

Abdus Salam International Centre for Theoretical Physics (ICTP), Trieste, Italy

(Manuscript received 6 August 2004, in final form 17 November 2004)

ABSTRACT

The atmospheric energy transport variability associated with decadal sea surface temperature variability in the tropical Pacific is studied using an atmospheric primitive equation model coupled to a slab mixed layer. The decadal variability is prescribed as an anomalous surface heat flux that represents the reduced ocean heat transport in the tropical Pacific when it is anomalously warm. The atmospheric energy transport increases and compensates for the reduced ocean heat transport. Increased transport by the mean meridional overturning (i.e., the strengthening of the Hadley cells) causes increased poleward energy transport. The subtropical jets increase in strength and shift equatorward, and in the midlatitudes the transients are affected. NCEP–NCAR reanalysis data show that the warming of the tropical Pacific in the 1980s compared to the early 1970s seems to have caused very similar changes in atmospheric energy transport indicating that these atmospheric transport variations were driven from the tropical Pacific. To study the implication of these changes for the coupled climate system an ocean model is driven with winds obtained from the atmosphere model. The poleward ocean heat transport increased when simulated wind anomalies associated with decadal tropical Pacific variability were used, showing a negative feedback between decadal variations in the mean meridional circulation in the atmosphere and in the Pacific Ocean. The Hadley cells and subtropical cells act to stabilize each other on the decadal time scale.

1. Introduction

Both the atmosphere and ocean transport energy poleward in the global climate system. The reanalysis data of the National Centers for Environmental Prediction–National Center for Atmospheric Research (NCEP–NCAR; Kalnay et al. 1996) shows that the contribution of the ocean and atmosphere to the total energy transport is of same order of magnitude in the Tropics (Trenberth and Caron 2001). In the tropical atmosphere, meridional overturning cells and monsoon circulations are the most important agents of transporting energy poleward. Diabatic heating occurs in the

rising branch of the Hadley cell, while adiabatic warming in the sinking branch is balanced by radiative cooling. This forces a poleward transport of dry static energy while the equatorward transport of moisture in the trade wind regions cause latent energy to be transported equatorward. However, the total transport of energy is poleward. The zonal asymmetries associated with the monsoons and subtropical highs also contribute to transport of energy. In the midlatitudes, the transient eddy transports in the storm track regions are the main contributors to the poleward energy transport. The contribution of these different terms in the heat budget has been subject of study since sonde data has been available. Peixoto and Oort (1992) summarize the contributions of the different processes using in situ data and top-of-the-atmosphere radiation. Zhang and Rossow (1997) give estimates based on surface heat fluxes and top-of-the-atmosphere radiation. New esti-

Corresponding author address: W. Hazeleger, Royal Netherlands Meteorological Institute (KNMI), P.O. Box 201, 3730 AE, De Bilt, Netherlands.
E-mail: hazelege@knmi.nl

mates are given by Trenberth and Stepaniak (2003) based on reanalysis data.

In the ocean, the wind-driven subtropical cells play an important role in the poleward energy transport in the Tropics. The Ekman-driven divergence at the equator drives upwelling and poleward transport of surface water. In the subtropics, Ekman pumping and subduction drives the water downward. In the interior, the water flows nearly adiabatically back to the equator (McCreary and Lu 1994). Model studies of tropical Pacific heat transport demonstrate that the horizontal gyres contribute to the heat transport as well. Warm water is transported at the western boundaries toward the equator, while relatively cold water flows poleward in the central and eastern parts of the basin. So the gyres transport heat toward the Tropics, but the amplitude is less than the heat transport by the subtropical cells (Hazeleger et al. 2004).

Apart from seasonal variations, it is less well known how energy transport varies in the climate system. It is difficult to obtain interannual or even decadal variations in energy transport from the reanalysis data. Changes in observation systems cause the time series to be inhomogeneous. Also, the satellite data that are used to estimate the radiation balance at the top of the atmosphere have a relatively short record. The observational records for the oceanic heat transports are very short. Oceanographers rely on hydrographic sections obtained from dedicated cruises or data from a sparse number of moorings to obtain estimates of oceanic heat transport (e.g., Talley 2003). Also, inverse modeling has helped to get estimates of heat transport using these observations (Ganachaud and Wunsch 2000).

Wielicki et al. (2002) and Chen et al. (2002) recently suggested, on the basis of satellite and atmospheric observations, that the total poleward energy transport by atmosphere and ocean in the Tropics varies on decadal time scales. It is well known that atmosphere and ocean energy transports vary during the ENSO cycle with increased poleward transport in both atmosphere and ocean during El Niño (Zebiak 1989; Sun 2000). This occurs as part of a transient phenomena involving heat exchange between atmosphere and ocean over years. On decadal time scales the upper ocean is expected to be more closely in equilibrium with the atmosphere forcing but it is not clear how the energy transports vary on these longer time scales. McPhaden and Zhang (2002) have claimed that there was less poleward mass export in the tropical Pacific Ocean by the meridional overturning during the 1990s. They suggest that this goes hand in hand with reduced poleward ocean heat transport consistent with warmer tropical sea surface temperatures (SSTs).

If the ocean heat transport varies as suggested by McPhaden and Zhang we need to know how the atmosphere energy transport varies. Held (2001) has argued that the partitioning between the tropical atmosphere and ocean energy transport remains fixed because both are associated primarily with meridional overturning, which is tied to the surface wind stress. If so then, if the ocean poleward heat transport reduces, the atmospheric energy transport should reduce too. That could only occur if the net top-of-the-atmosphere radiation balance changes. On the other hand, Bjerknes (1964) and Marshall et al. (2001) have argued that the net top-of-the-atmosphere radiation balance is tightly constrained such that the atmosphere and ocean energy transports should change so as to compensate for each other.

Compensating energy transports are indeed found in model experiments in which the ocean heat transport is forced to vary (Winton 2003; Clement and Seager 1999). However, Clement and Seager (1999) used either an idealized box model, ignoring the gyre circulation, or a general circulation model without dynamical coupling where all the ocean heat transport was removed. Winton (2003) used a general circulation model in which he changed the strength of ocean currents without dynamical coupling. So the question of how the atmosphere and ocean energy transports vary on longer time scales, when equilibrium is close to being established under full dynamical and thermodynamical coupling, remains open. A firmer understanding of this would allow an improved understanding of the atmosphere–ocean coupling that underlies decadal variability in the Tropics. In a previous study Hazeleger et al. (2004) used an ocean general circulation model to study how the ocean heat transport responds to persistent El Niño-like and La Niña-like wind stress forcing. For example, for persistent El Niño-like forcing, they found that the poleward ocean heat transport by the meridional overturning circulation decreased but was nearly compensated for by a decrease in the equatorward heat transport by the gyre circulation. Since, consistent with McPhaden and Zhang (2002), the total poleward heat transport decreased this was a positive feedback that would warm equatorial SSTs. Thus, the ocean heat transport feedback on SST has different signs for interannual and decadal wind stress forcing. This is possible because much of the interannual ocean heat transport variations are adiabatic changes in tropical thermocline depth.

If on decadal time scales warm equatorial SSTs are associated with reduced ocean heat export away from the equator, what stabilizes the coupled system? Does the atmospheric energy transport increase or does the

atmospheric response to decadal warming involve surface stresses that increase the ocean heat transport? In this study we will address these questions. First, we will examine the atmospheric energy transport response in a coupled atmosphere–ocean model to imposed changes in ocean heat transport. Second, we will take the surface winds from this experiment and examine the ocean heat transport response to them. These experiments attempt to examine the coupled system in a step-by-step way. Hopefully such partial-coupling experiments will be useful in understanding experiments with fully coupled models. It will be shown that the response of each fluid to energy transport variations in the other is compensatory, which will restrict the amount by which the top-of-the-atmosphere radiation can change. This is presumably a fundamental way in which the climate system is regulated.

2. Experimental setup

a. The models

The model that is used here is nicknamed SpeedO. It is a flexible coupled climate model that consists of a primitive equation atmosphere model which is configured with seven vertical layers and with spectral truncation at wavenumber 30 (Speedy) and a hierarchy of ocean models. The atmosphere model has simplified physics parameterization schemes, which ensures a large computational efficiency. A five-layer version of the Speedy atmosphere model is described by Molteni (2003). The current seven-layer version is an improvement and is described and validated in Hazeleger et al. (2003). A change has been made in the cloud scheme as described in the appendix. The atmosphere model is coupled to a slab mixed layer model forced by surface heat fluxes and a simple ice model. The temperature equation of the slab model is

$$\frac{\partial T}{\partial t} = \frac{1}{\rho c_{pv} h} (Q + \text{OHT}). \quad (1)$$

Here T is the temperature; h is the mixed layer depth, which has been taken constant at 80 m; ρ is the density of seawater; c_{pv} is the heat capacity of water; Q is the sum of the latent, sensible, and radiative surface fluxes; and OHT is an implied divergence of ocean heat transport. The latter term is specified such that the SST stays near its climatological value. The OHT is diagnosed from a run with the atmosphere model with prescribed climatological SST as the lower boundary condition. When SST and its tendency are specified, Eq. (1) can be used to diagnose OHT using the simulated Q . This heat flux is called a “ q flux.” It accounts for both the true

OHT and the errors in the modeled surface heat fluxes. Finally, a simple energy conserving land bucket model is used.

Implications for the coupled climate system are studied by forcing an ocean model with winds derived from the atmosphere model. We use the same primitive equation ocean model as used by Hazeleger et al. (2004). The model has a resolution of 2.5° by 2.5° in the midlatitudes and the resolution increases in the meridional direction to 0.5° at the equator. The domain covers the Pacific and Indian Ocean basins and ocean thermodynamic properties are restored to observations at meridional boundaries. The ocean model is coupled to an atmospheric mixed layer model such that the surface heat fluxes are internally computed (Seager et al. 1995). The wind stresses and wind speed are prescribed as well as fractional cloudiness and solar radiation. Details on the model can be found in Hazeleger et al. (2004, and references therein).

b. The experiments

To study the response of the atmosphere to decadal-like El Niño–Southern Oscillation (ENSO) variability we perform a control run and a run with perturbed ocean heat transport convergence with the thermodynamically coupled model. The experimental setup is very similar to that of Sutton and Mathieu (2002). First, the surface heat fluxes are diagnosed from a 100-yr run with the atmosphere model with prescribed climatological SST. In steady state these surface heat fluxes balance the implied ocean heat transport divergence [see Eq. (1)] and the climatological q flux is diagnosed from the prescribed tendencies and the simulated surface heat fluxes. These q fluxes are added to the temperature tendency equation in the slab mixed layer model to represent the ocean heat transport. This procedure ensures that the SST in the thermodynamically coupled model stays close to the climatological SST. The thermodynamically coupled model was run for 100 yr to obtain statistical significant responses (the control experiment).

To represent decadal variations in the tropical Pacific Ocean we ran the atmosphere model with the prescribed climatological SST plus an added SST perturbation typical for decadal ENSO. The SST perturbation that has been used is shown in Fig. 1a. The perturbation is obtained from a regression of SST anomalies on a filtered (10-yr running mean) time series of SST anomalies in the Niño-3 region using reanalysis data from 1949 to 2002. The amplitude of the pattern has been enhanced by a factor of 2 to get a clearer response in the atmosphere. After running the atmosphere model for 100 yr with this SST perturbation added to

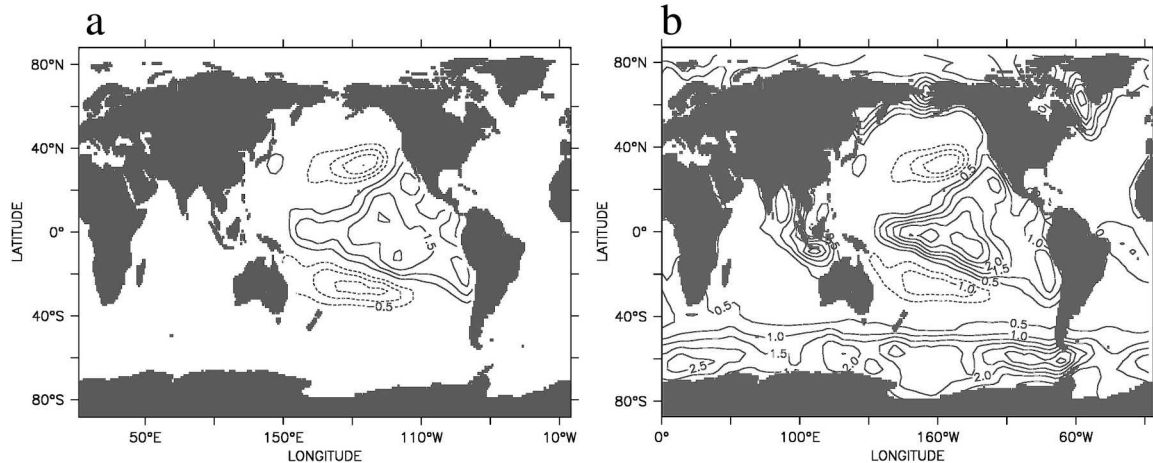


FIG. 1. (a) SST (K) pattern used as anomalous SST forcing in the spinup of the SST-forced atmospheric model to derive the anomalous q flux. (b) Difference of SST (K) in the DECENSO and control experiments.

the SST climatology we diagnosed the q fluxes. The difference between the implied poleward oceanic heat transport in the latter experiment and the experiment with only climatological SST as boundary condition is shown in Fig. 2. In response to the heating in the tropical Pacific, the implied ocean heat transport decreases by as much as 0.3 PW. This is consistent with the notion that a warmer tropical Pacific implies less heat transport by the ocean from the Tropics to the Poles. With the q flux thus obtained, we performed a second experiment with the atmosphere model coupled to the slab ocean mixed layer for 100 yr (the DECENSO experiment).

3. Results

a. Surface fields and circulation

Here we discuss the results from the simulations with Speedy coupled to the slab mixed layer. The results that are shown are obtained from the last 95 yr of the simulations. The first 5 yr are omitted to allow the atmosphere model, slab ocean model, and land model to spin up. The 95 yr are sufficient to obtain statistically stable results.

In response to the anomalous ocean heat transport associated with decadal ENSO, the model reproduces large SST anomalies in the tropical Pacific (Fig. 1b). Indeed, the pattern of the SST anomalies is reminiscent of the warm phase of the decadal ENSO cycle. That is, there are large positive anomalies in the central tropical Pacific and negative anomalies in the subtropics and midlatitudes. The SST anomalies are slightly larger than the prescribed anomalies that were used to derive the anomalous q fluxes. Positive anomalies are found in the Southern Oceans and in the Arctic regions. As this

is remote from the initially applied SST perturbation, a change in atmospheric circulation must have generated these anomalies. The mechanism to get such a remote response will be discussed later although we will focus on the Tropics. Note that the thermodynamically coupled model has more degrees of freedom than the model with prescribed SST and we do not expect to find the same solution in the q -flux runs and SST-forced runs.

The zonal mean circulation strengthens when anoma-

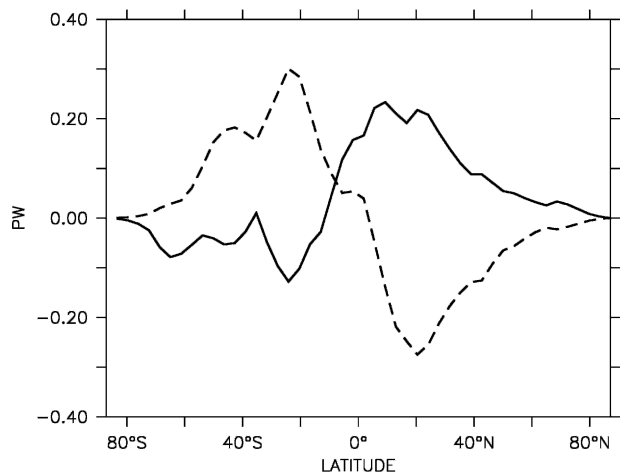


FIG. 2. Anomalous implied northward ocean heat transport (dashed) and anomalous implied atmospheric heat transport (continuous) as derived from the surface heat fluxes over sea and the top-of-the-atmosphere radiation from the experiment with the atmosphere model coupled to the slab model with climatological q flux and the atmosphere model coupled to the slab model with prescribed q -flux anomaly included related to decadal ENSO (in $\text{PW} = 10^{15}\text{W}$). The anomalous ocean heat transport is by definition identical to the anomalous heat transport associated with the decadal ENSO pattern as derived from the spinups with prescribed SSTs.

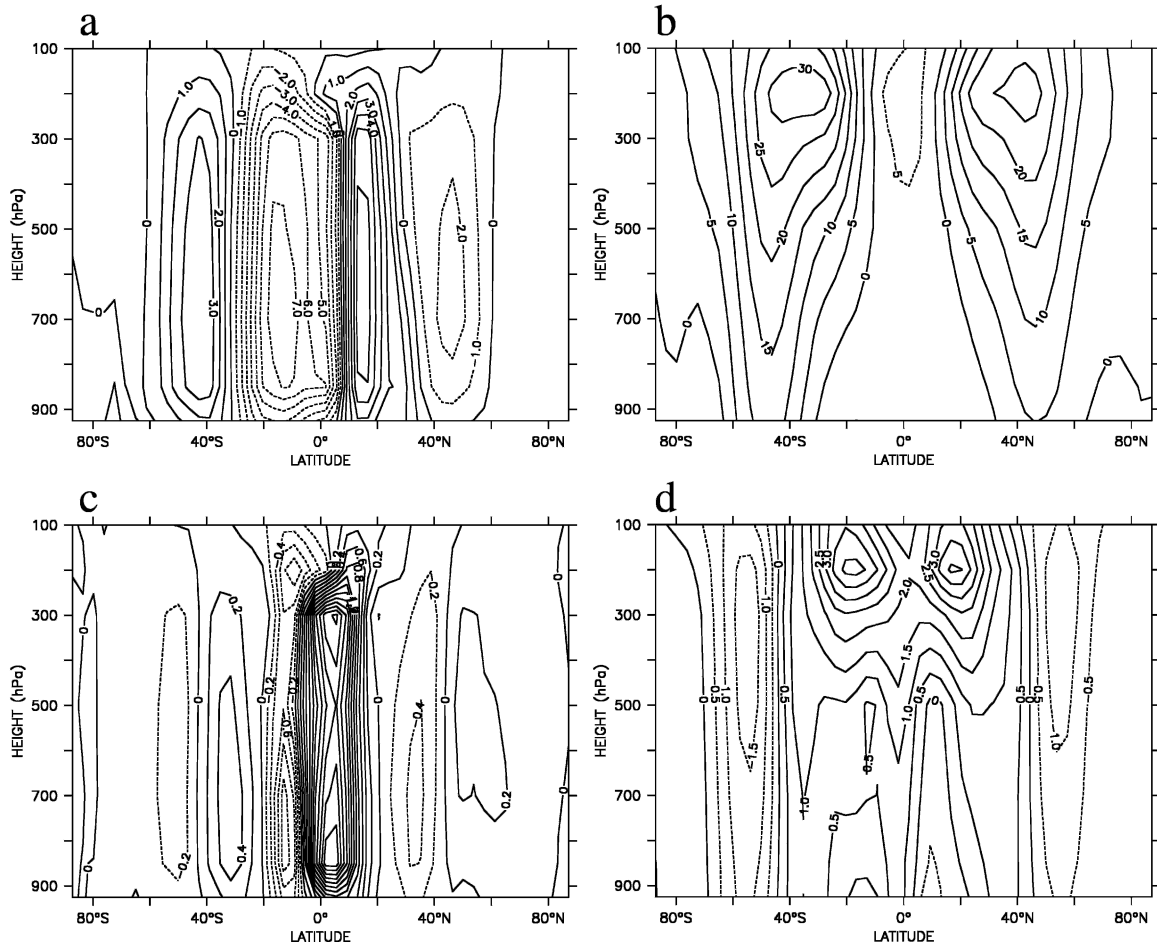


FIG. 3. (a) Meridional mean overturning circulation in the atmosphere ($10^{10} \text{ kg s}^{-1}$). (b) The zonally averaged zonal winds (m s^{-1}). (c) The difference between the meridional mean overturning and (d) the difference between zonally averaged zonal winds in the DECENSO and control experiments.

lous q fluxes associated with decadal ENSO are applied. In response to the heating at the surface, the Hadley cells spin up (Fig. 3c) and the rising branch shifts southward toward the thermal equator while remaining north of the equator. Consequently, in a strip between 5°N and 5°S , where the zonal mean surface winds are northward, the surface winds decrease in strength, but outside that region the trades increase in strength. This rather subtle change will be important for the heat transport changes in the coupled climate (see section 4). As the zonal mean circulation intensifies, the subtropical jets strengthen and become more confined to the equator. This has been shown by Seager et al. (2003) for interannual variability associated with ENSO. Furthermore, the thermodynamic indirect cells in the midlatitudes enhance, suggesting changes in the transient eddy momentum fluxes in the midlatitudes. In accordance with the findings of Wielicki et al. (2002) and Chen et al. (2002) the cloudiness decreases in the

downwelling branch of the Hadley cells and shortwave radiation increases accordingly.

The model also captures the teleconnections associated with SST anomalies in the tropical Pacific realistically (Berlage 1966; Trenberth et al. 1998). The difference in geopotential height in the DECENSO and the control experiment shows the familiar wavelike pattern emanating from the Tropics to the extratropics and a rise of geopotential height in the Tropics, associated with the heating (Fig. 4a). In the North Pacific and over North America, the Pacific–North American (PNA) pattern is visible, while in the Southern Hemisphere, the Pacific–South American pattern (Liu et al. 2002) is well simulated. This response is very similar to the teleconnections associated with SST anomalies in the eastern tropical Pacific found in model runs with historical SST anomalies prescribed (Hazeleger et al. 2003). Here the remote response of geopotential height remains in response to steady forcing.

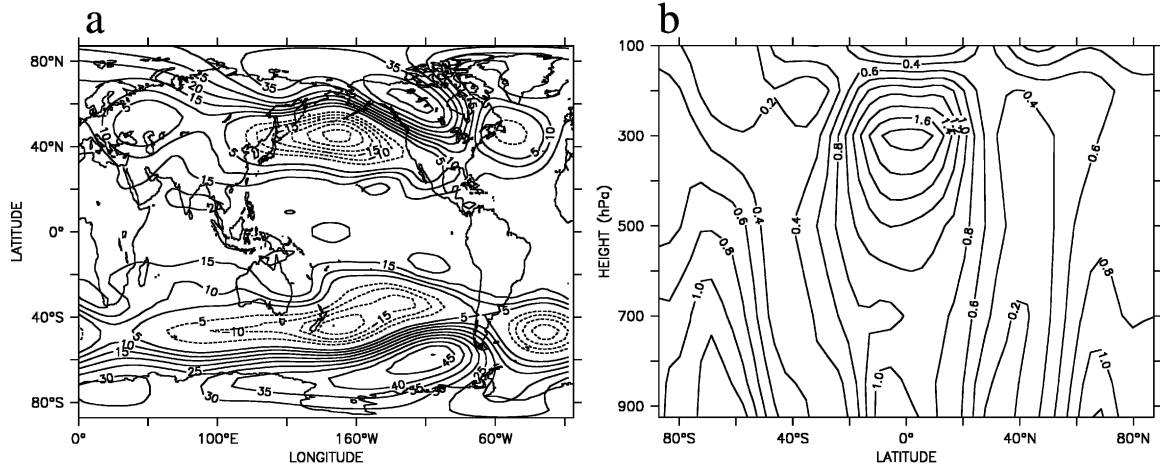


FIG. 4. (a) The difference between geopotential height (m) at 500 hPa and (b) the difference between zonally averaged temperature (K) in DECENSO and control experiments.

The change in the zonally averaged temperature shows that the largest changes occur in the upper troposphere in the Tropics (Fig. 4b). Here, the increase in the release of latent energy caused by increased convection creates positive temperature anomalies. In the lower troposphere, the anomalies are positive in the Tropics. Large anomalies in the high latitudes are also visible.

b. Energy transport

1) ZONAL AND VERTICAL INTEGRALS

We now turn to the energy transport in the atmosphere. As shown in Fig. 2, the atmospheric heat transport tends to compensate for changes in oceanic heat transport. This result has been found in other studies with a similar set up (Clement and Seager 1999). To gain more insight in the mechanisms that cause the compensation we decompose the total energy in the atmosphere into potential energy (P_E), internal energy (I_E), latent energy (L_E), and kinetic energy (K_E):

$$P_E + I_E + L_E + K_E = gz + c_p T + L_v q + \frac{1}{2}(u^2 + v^2). \quad (2)$$

Here g is the gravitational constant, z is the geopotential height, c_p is the heat capacity of dry air, T is the temperature, L_v is the latent heat of condensation, q is the specific humidity, and u and v are the horizontal velocities. In general the contribution of kinetic energy is small and will be discarded from now on. The mean meridional transport of energy can be further decomposed into the following (e.g., Peixoto and Oort 1992):

$$\begin{aligned} \overline{[gz + c_p T + L_v q]v} &= g[\overline{v}][\overline{z}] + g[\overline{v'z'}] + g[\overline{v^*z^*}] \\ &+ c_p[\overline{v}][\overline{T}] + c_p[\overline{v'T'}] \\ &+ c_p[\overline{v^*z^*}] + L_v[\overline{v}][\overline{q}] \\ &+ L_v[\overline{v'q'}] + L_v[\overline{v^*q^*}]. \end{aligned}$$

The square brackets denote the zonal average, the asterisks the deviation from the zonal averages, the bars denote the time average, and the primes the deviation from the time average. Using this decomposition, the energy transport is separated into transport by the mean meridional circulation (e.g., Hadley cells), a transport by quasi-stationary waves (e.g., subtropical anticyclones) and within-month transients (e.g., synoptic storms). In the following we will combine the potential and internal energy in a dry static energy ($gz + c_p T$). The atmospheric velocity that is used for determining the mean meridional circulation has been derived from the velocity potential (i.e., $v = \partial\chi/\partial y$, with χ the velocity potential). That is, only the divergent part of the velocity will be considered as that relates directly to diabatic forcing in the atmosphere. Calculations have been performed with monthly means and the primes denote the submonthly variations. Plots will be shown for the mass-weighted vertical and zonal integral of the energy transport and their anomalies.

The dry static energy transport by the mean meridional circulation shows a poleward energy transport in the Tropics and subtropics with maxima of 1.3 PW in the Northern Hemisphere and a minimum of -2.1 PW in the Southern Hemisphere (Fig. 5). This is consistent with the findings of Peixoto and Oort (1992), but somewhat lower than more recent estimates of Trenberth and Stepaniak (2003).

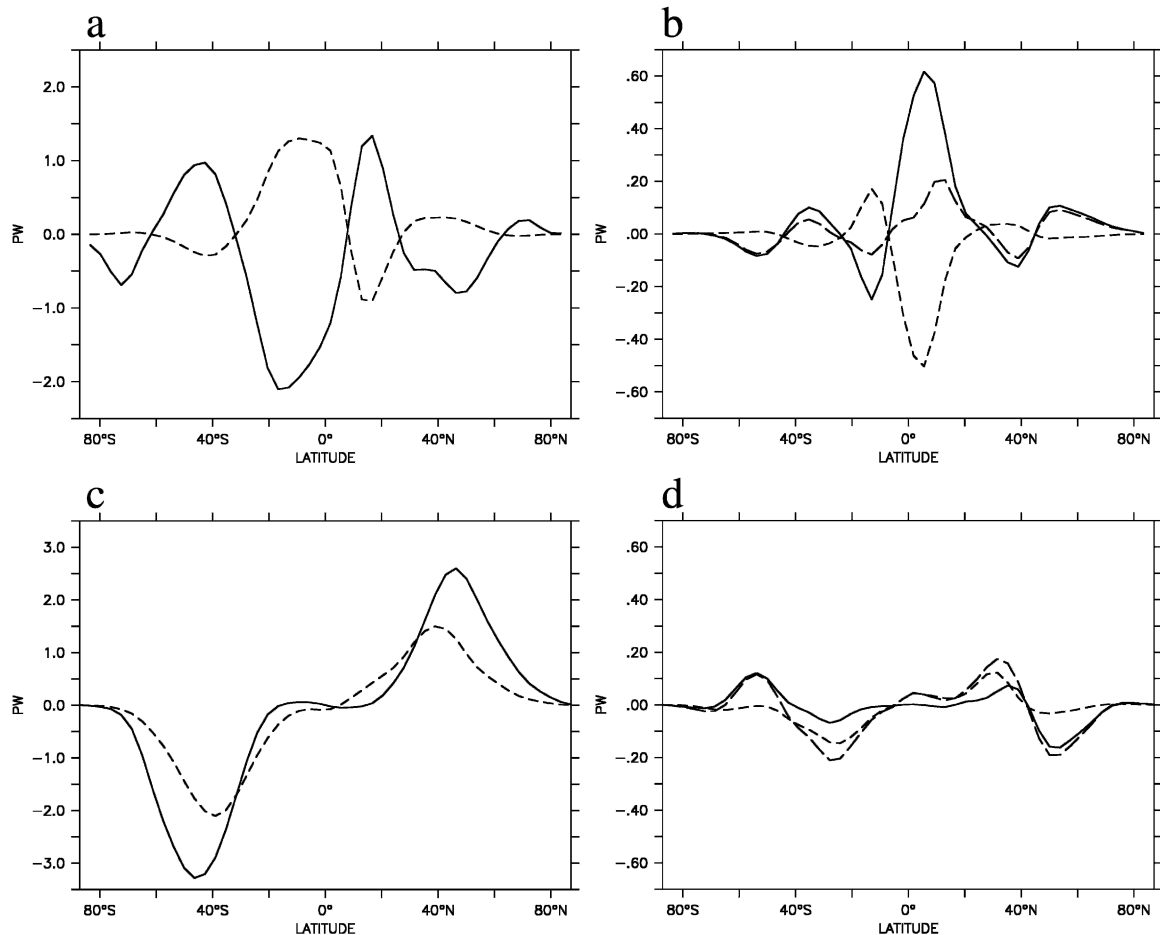


FIG. 5. Northward meridional dry static energy transport (continuous) and northward meridional latent energy transport (dashed) in PW ($=10^{15}$ W) (a) by mean meridional circulation; (b) the difference in northward energy transport by mean meridional circulation in the DECENSO and control experiments; (c) by the transient eddies; and (d) the difference in northward energy transport by transient eddies in the DECENSO and control experiments. In (b) and (d) the sum of the latent and dry static energy transport anomalies is also shown in long dashes.

In response to the reduced oceanic heat transport associated with decadal ENSO and the rise of tropical Pacific SST, the dry static energy transport by the mean meridional transport enhances by as much as 0.6 PW at 5° N (Fig. 5b). The anomalies in the latent heat transport are equatorward and opposite to the anomalies in dry static energy transport. These changes are especially clear just north of the equator, consistent with the increase of the Northern Hemisphere Hadley cell and its equatorward shift. Cross sections of anomalies in dry static energy transport show large anomalies in the Tropics near the surface and around 300 hPa in the deep Tropics where the latent heat is released while changes in latent heat take entirely place in the lower troposphere (not shown).

The net change in moist static energy ($gz + c_p T + L_v q$) by the mean meridional circulation peaks in the

Tropics around 15° N at about 0.2 PW. The tropical atmosphere closely compensates for the decreased oceanic heat transport, leaving only small changes in total heat transport. The increased overturning circulation in the atmosphere and stronger subtropical jets have previously been related to ENSO-like changes (see Seager et al. 2003) and are realistic. Note, however, that in the current setup the ocean is not able to dynamically adjust itself. In this experimental setup, the mass overturning in the ocean and atmosphere are not related to each other as envisaged by Held (2001).

The transient energy fluxes peak in the midlatitudes around 45° N and 45° S and transfer energy poleward (Fig. 5c). The amplitudes and structure are similar to the estimates of Trenberth and Stepaniak (2003). The moist static energy peaks at 4 PW in the Northern Hemisphere and 5.1 PW in the Southern Hemisphere.

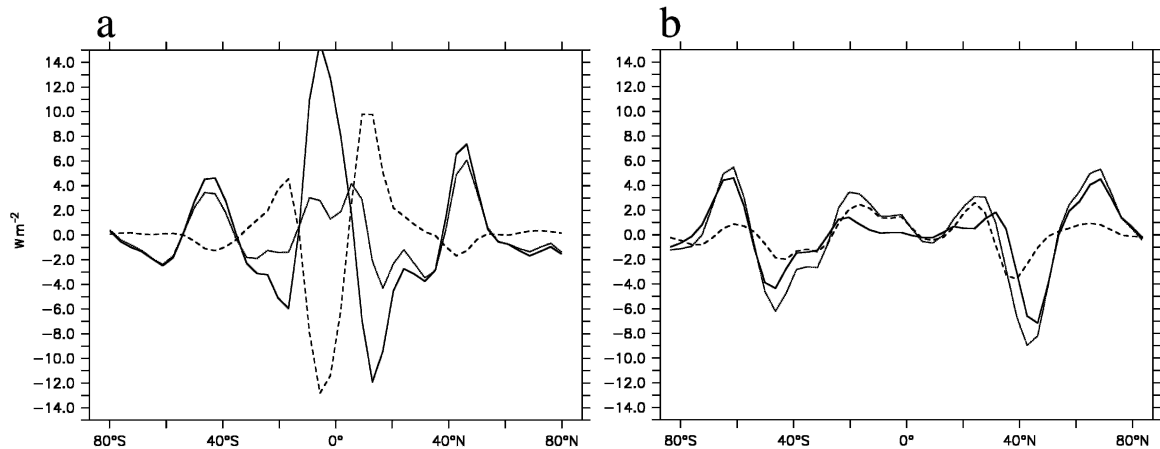


FIG. 6. Divergence of the energy transports in W m^{-2} (continuous: dry static energy, dashed: latent energy, dotted: moist static energy). The difference of contribution (a) by mean meridional circulation and (b) by transient eddies between the DECENSO and control experiments is shown.

The dry static energy transport is slightly larger than the latent energy transport and peaks more poleward. In the Tropics the contributions of the transients are very small. Anomalies in the transient energy transport are of the order of 0.1 PW. Although this is small compared to the mean transient energy transport, it is of the same order of magnitude as changes in energy transport by the meridional mean transport. The changes in dry static energy and latent energy transport are best described by an equatorward shift of the energy transports. Poleward of the maxima of the energy transports in the control run the transports decrease and equatorward they increase. The equatorward increase is especially clear in the latent heat transport anomalies. The shift is obviously related to an equatorward shift of the zonal winds. This shifts the region of high baroclinicity and the associated transients equatorward. As a result, the thermally indirect cells driven by the transient eddies are affected as well. Such changes and mechanisms are discussed in detail by Seager et al. (2003). Note that the energy transport by the meridional mean circulation and by the transient eddies are opposite and nearly compensate for each other in the midlatitudes.

The contribution of changes in energy transport by stationary eddies is rather small and not very coherent. Only the change in latent energy transport by stationary eddies is sizeable, that is, 0.2 PW at 20°N.

2) SOURCES AND SINKS

So far, we can conclude that the atmospheric energy transport compensates for the decrease in oceanic heat transport in a thermodynamically coupled model. In

the Tropics, the changes in the mean meridional circulation cause the compensation, in the subtropics and midlatitudes the changes in the transient eddies cause the compensation. There is also strong cancellation within the atmosphere. In the Tropics, the dry static energy transport and the latent energy transport by the mean meridional circulation tend to cancel. In the midlatitudes, the energy transport by the transients and the energy transport by the transient, eddy-driven meridional mean circulation compensate to a large degree. The implications of changes in the energy transport become more clear when the divergences are compared. The divergences of the energy transports show the sources and sinks of energy.

In Fig. 6a we show the changes in divergences of the moist static energy due to the changes in the meridional mean circulation and zonal mean energy. The figure shows that the changes in the meridional mean circulation acts to diverge heat away in the tropical areas balancing the increased diabatic heating associated with higher SSTs and increased surface evaporation. In the midlatitudes the transient eddy fluxes converge heat, which is largely balanced by the divergence by the meridional mean circulation (Fig. 6b). Were there no diabatic heating anomaly these two would exactly cancel each other out (Andrews et al. 1987).

In the deep Tropics the mean meridional circulation is the most important component of the total heat transport. The transients become important in the subtropics and their contribution peaks in the midlatitudes where energy transport by the meridional mean circulation and the transient eddies tend to compensate. This is expected given that the mean meridional circulation in the midlatitudes is primarily eddy driven.

4. Discussion

a. Comparison to observations

We showed that the atmospheric energy transport tends to compensate for variations in oceanic heat transport in a thermodynamically coupled model. Although the atmosphere has its own regulation of compensating energy transports (e.g., near cancellation of latent and dry static energy transport in the Tropics), the atmospheric energy transport went up when the oceanic heat transport went down, especially in the Tropics. Changes in the mean meridional circulation were responsible for the compensation in the Tropics.

Many changes in the circulation that are presented here have resemblances to changes associated with the interannual ENSO phenomenon. That is, during the warm phase of ENSO the Hadley cells strengthen and the rising branch moves equatorward. Also, the changes in the upper-tropospheric winds are similar to the hemispheric symmetric response to El Niño found in observations (see Seager et al. 2003). Seager et al. also found changes in the transient eddies in the mid-latitudes associated with ENSO, arguing that the equatorward shift of eddy-induced vertical motion causes cooling in the midlatitudes. This cooling is not found, but the warming is at a minimum here. Finally, the teleconnection patterns are very similar to observed teleconnection patterns associated with the El Niño phenomenon. However, by applying steady perturbations and studying the time mean response over many decades we show that these responses can persist.

Although the simultaneous presence of changes in the observation network, anthropogenic change, and natural variability make the decadal changes in the reanalysis data hard to interpret, we show the differences in atmospheric heat transport between two decades: 1978–87 and 1967–76. The later decade was relatively warm in the tropical Pacific and the early decade relatively cold representing opposite phases of decadal ENSO or the Pacific decadal oscillation (Mantua et al. 1997; Zhang et al. 1997). The observed SST difference between the two periods is reminiscent of the pattern used in the model experiments discussed before. Again, we use the divergent meridional velocity for determining the mean meridional transports. The transient eddy contribution of internal energy transport ($\overline{v'z'}$) is not part of the reanalysis dataset, but the contribution will be small as transient eddies are quasigeostrophic to good approximation (Peixoto and Oort 1992). Note that we use the fields from the reanalysis data without additional corrections. Such corrections are applied by Trenberth and Caron (2001), but are beyond the scope of this paper.

The atmospheric energy transport changes are shown in Fig. 7 and can be readily compared to the simulated anomalies in energy transports in Fig. 5. The northward transport of dry static energy by the mean meridional circulation in the Tropics is much stronger when the tropical Pacific is anomalously warm. Just as in the model, the transport of latent energy mediates the poleward energy transport in the Tropics. These changes are driven by changes in the strength of the Hadley circulation as shown in Fig. 7c. The Hadley circulation became stronger in the late 1970s and early 1980s and its rising branch moved equatorward. Also, the changes in the energy transport by the transient eddies bears some similarity to those simulated, especially in the Southern Hemisphere. The decrease in dry static energy transport around 50°N that was found in the model is not found in the reanalysis data. The changes in the transient eddy fluxes are related to changes in the storm tracks. In response to the tropical heating the storm tracks move equatorward in the Pacific in the model (Fig. 8). Similar changes are reported by Chang and Fu (2002). They suggest that observed storm track variations on the interdecadal time scale are related to decadal SST changes in the tropical Pacific. The hemispherically symmetric increase in the strength of the subtropical jets and the shift in their position is not well observed in these decadal differences, although it shows up clearly on interannual time scales (not shown).

The rough similarity of these changes to those in the experiments with reduced ocean heat transport suggests that the observed decadal changes in atmospheric circulation were in part driven by warming of the tropical Pacific. However, definite conclusions cannot be drawn from the reanalysis data because of the quality of the data, especially because the changes in the observational network might have influenced these results. It is noteworthy to mention that the results obtained from the reanalysis data are sensitive to the period that is chosen. When longer time periods are considered, changes in the Southern Hemisphere become dominant; these are signatures of trends in the Southern Annular Mode. When the 1990s are compared to the 1970s there is a strong increase in the winds around Antarctica in conjunction with large changes in the energy transport driven by transient eddies. These changes are probably driven by changes in radiative forcing due to the increase of greenhouse gasses (Kushner et al. 2001).

b. Implication for the coupled climate system

To understand the implications for the coupled climate we need to address how this change in atmospheric circulation will subsequently impact the ocean

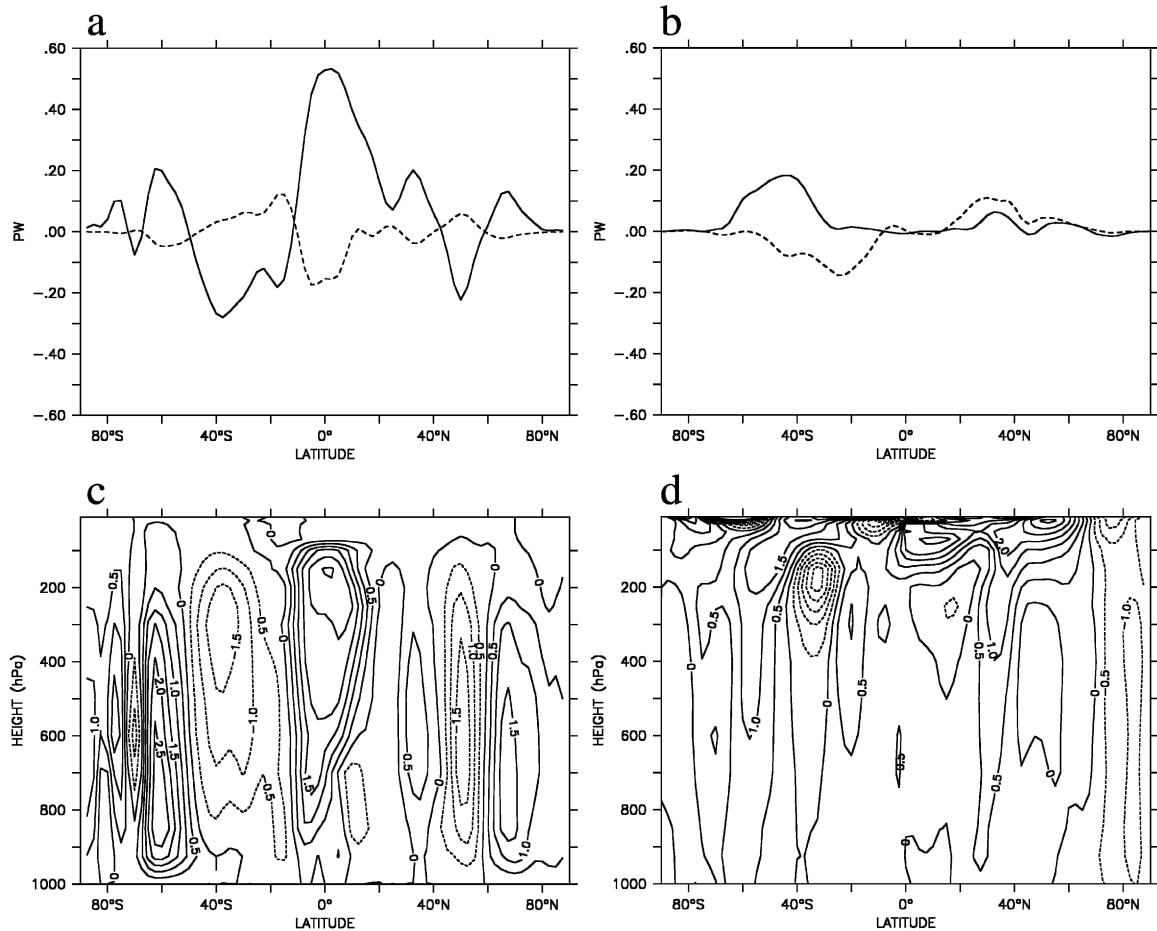


FIG. 7. Changes (1978–87 minus 1967–76) in meridional dry static energy transport (continuous) and meridional latent energy transport (dashed) in PW in the NCEP–NCAR reanalysis data by (a) mean meridional circulation and (b) by the transient eddies. (c) The change in meridional mean streamfunction ($10^{10} \text{ kg s}^{-1}$). (d) The change in zonal mean winds (m s^{-1}).

heat transport. Is there a positive or negative feedback? As we have seen, the response of the atmosphere to a reduction of ocean heat transport is a spinup of the Hadley cells. The oceanic response will depend mainly on the zonal wind stress. The zonal wind stresses drive poleward Ekman transport near the equator and generate subtropical cells, which carry most of the poleward ocean heat transport in the Tropics. Depending on the location of the heating anomalous easterlies (east of the heating) or anomalous westerlies (west of the heating) can be generated (Gill 1980). Therefore, it is hard to predict a priori how the oceanic heat transport changes associated with these wind stress changes. As shown by Hazeleger et al. (2004) it depends on details of changes in the zonal wind stress, the curl of the wind stress, and on the distribution of the SST, all of which depend on the location of the heating. It was also found that a substantial amount of heat is carried by the geostrophic flow and the western boundary currents,

which were not included in the conceptual model of Held (2001).

The atmospheric model simulates a reduced zonal wind stress on the equator and increase of the wind stress around 10°N and 10°S (Fig. 9a). The pattern of the changes in the wind stress are very similar to that obtained from observations by McPhaden and Zhang (2002). That is, the anomalous northwestward wind from 160°E to 160°W at 15°S and the southeastward wind anomalies just to the north of that patch are found in the reanalysis data as well. These wind changes are associated with an equatorward shift of the South Pacific convergence zone. However, the weakening of the traders near the equator, indicated by the eastward anomalies, has a much broader structure in the observations. This might be due to the relatively coarse resolution of the atmosphere model or parameterizations of convection. The change in the curl of the wind stress shows a clear equatorward shift of the major patterns.

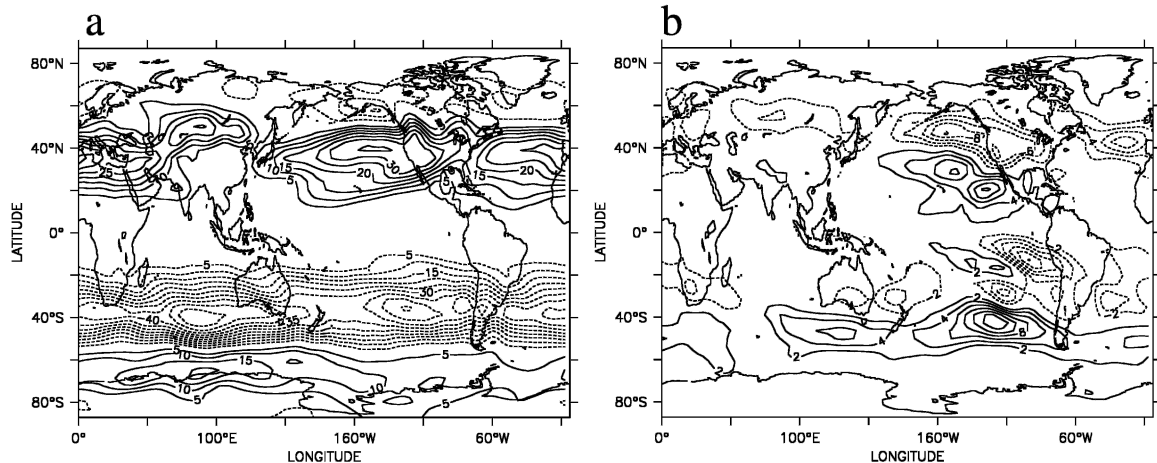


FIG. 8. Transient momentum flux $\overline{u'v'}$ at 300 hPa: (a) the control experiment and (b) DECENSO minus the control experiment ($\text{m}^2 \text{s}^{-2}$).

Figure 9b shows the Ekman transport as derived directly from the wind stresses in the DECENSO and in the control experiments. At the equator the Ekman transport reduces when the Pacific warms, indicating that weaker subtropical cells could be generated, which would be consistent with the weaker oceanic heat transport shown in Fig. 2. However, it is also possible that only the strengths of the more equatorially confined shallow tropical cells are primarily affected. Observations indicate a weakening of the subtropical cells when the SSTs are anomalously high in the tropical Pacific. However, the Ekman transport becomes stronger between 5° and 20°S and between 10° and 20°N . This differs significantly from McPhaden and Zhang (2002) who found a reduced Ekman transport at 9°N and 9°S ,

although the spatial pattern of the variations were rather similar. The pattern does differ from the one used by Hazeleger et al. (2004). They applied anomalous westerlies at the equator in the central Pacific to their model and found a reduction of the heat transport. Here the easterly wind anomalies are found more to the west and the off-equatorial wind anomalies are larger.

As argued before, it is hard to predict from the wind stress and the derived Ekman transports alone how the total ocean heat transport will change. Therefore, to test whether the simulated wind changes would act to further decrease the ocean heat transport or enhance it we conducted two experiments with the Lamont Ocean and Atmospheric Mixed Layer Model (LOAM) in a similar fashion as in Hazeleger et al. (2004). In the first

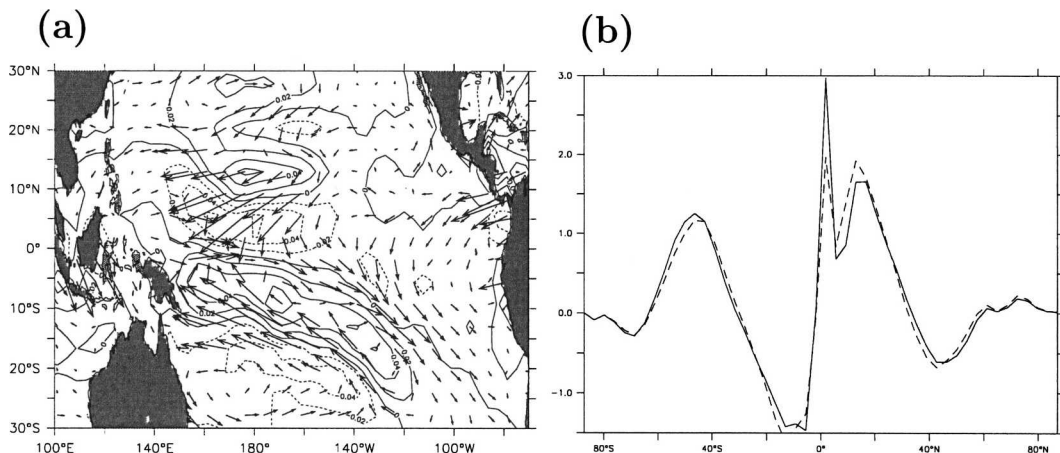


FIG. 9. (a) The difference in surface wind stress (vectors, largest vector 0.06 N m^{-2}) and curl of wind stress (contours) between the DECENSO and control experiments. (b) Zonal mean Ekman transport $\langle v \rangle = 1/[\rho_w(f^2 + r^2)](r\tau_y - f\tau_x)$; $\text{m}^4 \text{ s}^{-1}$ in the control (continuous) and DECENSO (dashed) experiments in the Pacific between 120°E and 90°W . The linear friction r is 1.5 day^{-1} and f is the Coriolis parameter.

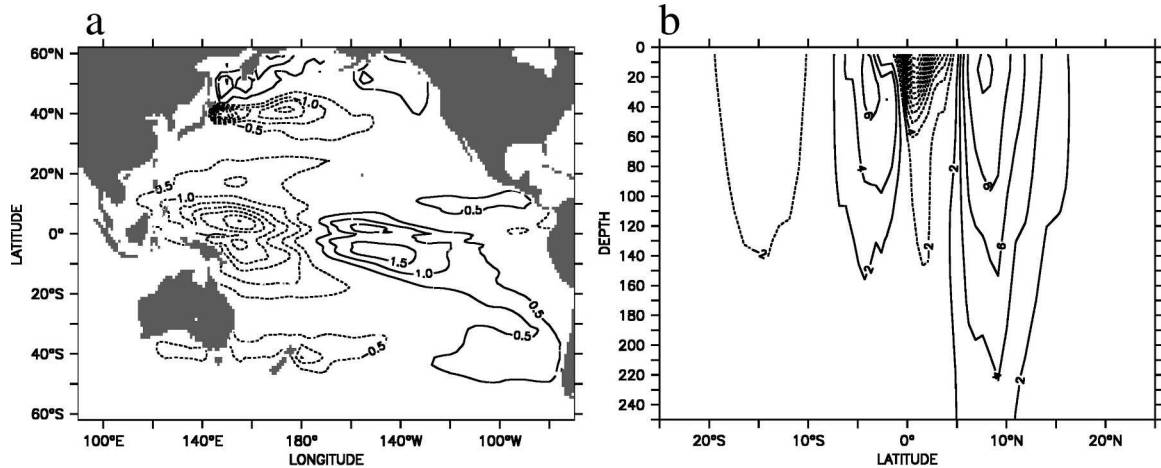


FIG. 10. (a) SST difference (K) in the ocean model with anomalous winds specified (see Fig. 9) and a control run with climatological forcing. (b) The difference in overturning streamfunction [Sv ($1 \text{ Sv} \equiv 10^6 \text{ m}^3 \text{ s}^{-1}$)] between the ocean model runs mentioned in Fig. 9.

experiment we forced the model with climatological winds. In a second experiment we added wind anomalies derived from the difference between the DECENSO and the control experiment of the atmospheric model. The experiments were run for 20 yr and the last 5 yr were used in the following analysis.

The SST response in the ocean model shows a warming of the central tropical Pacific and a cooling in the warm pool (Fig. 10a). Also, the Kuroshio region cools. In general, this is a typical response to El Niño-like wind anomalies. However, the well-observed warming in the eastern tropical Pacific is absent, while the cooling in the warm pool is much larger than observed during the positive phase of decadal ENSO variability. Also, the SST response of the ocean model to the wind anomalies is different from the SST anomaly applied to the atmosphere model in order to generate the wind anomalies (cf. Fig. 1 with Fig. 10). This may be due to model error or due to the unchanged cloud cover and solar radiation but, if the patterns are caused by coupled feedbacks, one would not expect these patterns to be the same as the atmosphere and ocean models are not coupled: the difference may contain the ocean's delayed response to the wind forcing.

The Eulerian mean overturning circulation in the ocean increases in magnitude in the subtropics, but it decreases near the equator (Fig. 10b, the mean overturning of this model has been shown by Hazeleger et al. 2001b, their Fig. 12a). The decrease near the equator is not very important for this study as the strong tropical cells close to the equator do not carry much heat (e.g., Hazeleger et al. 2001a). The off-equatorial increase of the overturning mass transport is more important for the changes in ocean heat transport. Consequently, the ocean heat transport increases when the

anomalous winds from the DECENSO experiment are added to the climatological winds, the exception being a small region between 0° and 5°N .

In general, the simulated anomalous winds associated with the DECENSO SST anomaly ultimately act to increase poleward energy transport in the ocean (Fig. 11). This shows that a negative feedback is operating by which the subtropical cells will cool the tropical oceans after a warm period. The results of this study and the study of Hazeleger et al. (2004) indicate ENSO-like winds can act to decrease the ocean heat transport and warm the tropical Pacific. In response, the atmospheric heat transport increases and the off-equatorial wind response leads to an increase in the strength of the subtropical cells, which will damp the warming in the tropical Pacific, suggesting a coupled negative feed-

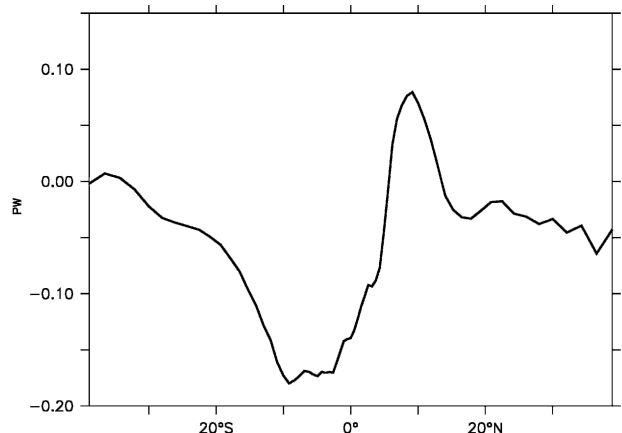


FIG. 11. The difference between northward ocean heat transport (PW) in the ocean model with anomalous winds from the atmosphere model associated with DECENSO added (Fig. 9a) and an ocean model with climatological forcing.

back. This circular argument indicates that coupled feedbacks are operating. However, we need to be careful, as the model deficiencies cause the simulated winds to be different from the observed winds. Also, Hazeleger et al. (2004) used an El Niño-like wind pattern that has small amplitude in the subtropics, while the observed decadal wind variations and simulated winds have a larger amplitude in the subtropics. However, the increased off-equatorial winds are found both in the model and in the observations and can lead to increased strength of the subtropical cells (Klinger et al. 2002).

The results are in line with the findings of Nonaka et al. (2002) who found that off-equatorial winds cause a lagged response at the equator, although they could not investigate the subsequent atmospheric response and identify whether a positive or negative feedback would be operating. Aspects of this study are in accordance with the study of Held (2001). The increased meridional mean circulation in the atmosphere increases the shallow overturning cells in the ocean. However, in this study it is the reduced oceanic heat transport, and presumably the shallow overturning and associated warming of the Tropics, which generates the increased atmospheric heat transport. This results in a possibility of coupled oscillatory behavior in a similar fashion to what was suggested in a conceptual model by Gu and Philander (1997). However, they envisaged that advection of subsurface temperature anomalies are generating changes in heat transport. Here, changes in overturning transport seem more important. The minor role of advection of subsurface temperature anomalies and the more important role of variations in volume transport is consistent with studies of, for instance, Schneider et al. (1999), Hazeleger et al. (2001c), and Kleeman et al. (1999).

5. Conclusions

We coupled a thermodynamic slab mixed layer to a primitive equation atmosphere model and showed that the atmospheric energy transport increased when the prescribed oceanic heat transport in the slab mixed layer reduced. The implied reduced ocean heat transport is consistent with estimates from observations of that which occurs with decadal variations of ENSO. The effect of the decreased heat transport by the ocean causes the SSTs to warm up, the Hadley cells to spin up and the subtropical jets to shift equatorward. The rise of atmospheric energy transport in response to reduced oceanic heat transport is accommodated by an increase of the energy transport by the mean meridional circulation in the Tropics in the model. The transient eddy fluxes in the midlatitudes change accordingly as they depend on the background circulation (see Seager et al.

2003). These changes are comparable to decadal changes in circulation and energy transport found in the NCEP-NCAR reanalysis data associated with decadal shifts in the SST in the tropical Pacific. When the circulation and energy transports from 1977 to 1987 are compared to those in the period from 1967 to 1976, comparable changes in the mean meridional circulation and transient eddy fluxes are found. So, it is likely that these observed changes were driven by the warming of tropical Pacific SST. For longer periods a different picture emerges from the reanalysis data, probably caused by changes in radiative forcing added to the natural variability.

The consequences for the coupled climate system were determined by studying changes in the Ekman transport and the response of an ocean model to the anomalous winds simulated in the atmosphere model. When the Hadley cells spin up in response to the warming in the tropical Pacific, the trades away from the equator strengthen, but the zonal wind stresses in the warm pool weaken. Consequently, the strength of the overturning cells in the ocean decreases close to the equator, but increases in the subtropics. The response of the ocean heat transport in the ocean model shows that the off-equatorial increase has a bigger impact and the poleward ocean heat transport increases. This indicates a negative feedback between tropical Pacific ocean-atmosphere variations at low frequencies. The Hadley cells and subtropical cells act to stabilize each other on the decadal time scale.

These mechanisms need to be tested in dynamically coupled ocean-atmosphere models. Subtle details such as the exact location of the heating ultimately determine the dynamical response of the atmosphere and ocean. A shift of the heating toward the central Pacific would result in different wind stress and SST response, and hence a different ocean heat transport response. The different ocean response to the wind anomalies derived from an atmospheric model, which was driven by SST itself, shows that coupled processes are important.

Acknowledgments. We thank Naomi Naik for support to obtain the results from the LOAM runs. Richard Seager was supported by NSF Grant ATM-9986072 and NOAA Grants UCSIO CU 02165401 and NA16GP2024.

APPENDIX

A Cloud Scheme

A five-layer version of the atmosphere model used here has been described by Molteni (2003). The current

model has two extra layers and a different cloud scheme compared to that model. In the current scheme the fractional horizontal area of a grid box covered with clouds is

$$c = \left(\frac{R/F - R_0}{1 - R_0} \right)^2 + \alpha \sqrt{P}. \quad (\text{A1})$$

Here R is the relative humidity, R_0 is a threshold humidity, and F is a parameter that is 1.0 over land and sea ice, while it is a function of the vertical velocity at 700 hPa such that F is smaller at descending motions, and F is a function of the temperature difference between the surface and at 850 hPa. Here P is the precipitation and α a constant factor. Finally, the threshold relative humidity at which clouds form has a vertical profile:

$$R_0 = R_{\text{top}} + (R_s - R_{\text{top}})[1 - e^{1-(p/p_s)^{-4}}]. \quad (\text{A2})$$

Here, R_s is a specified surface value of 0.3, R_{top} is 0.99, and p and p_s are the pressure and surface pressure, respectively.

REFERENCES

- Andrews, D. G., J. R. Holton, and C. B. Leovy, 1987: *Middle Atmosphere Dynamics*. International Geophysics Series, Vol. 40, Academic Press, 489 pp.
- Berlage, H. P., 1966: The Southern Oscillation and world weather. Mededelingen en Verhandelingen, No. 88, KNMI, 152 pp.
- Bjerknes, J., 1964: Atlantic air/sea interaction. *Advances in Geophysics*, Vol. 10, Academic Press, 1–82.
- Chang, E. K., and Y. Fu, 2002: Interdecadal variations in Northern Hemisphere winter storm track intensity. *J. Climate*, **15**, 642–658.
- Chen, J., B. E. Carlson, and A. D. Del Genio, 2002: Evidence for strengthening of the tropical general circulation in the 1990s. *Science*, **295**, 838–841.
- Clement, A. C., and R. Seager, 1999: Climate and the tropical oceans. *J. Climate*, **12**, 3383–3401.
- Ganachaud, A., and C. Wunsch, 2000: Improved estimates of global ocean circulation, heat transport and mixing from hydrographic data. *Nature*, **408**, 453–457.
- Gill, A. E., 1980: Some simple solutions for heat induced tropical circulation. *Quart. J. Roy. Meteor. Soc.*, **106**, 447–462.
- Gu, D., and S. G. H. Philander, 1997: Interdecadal climate fluctuations that depend on exchanges between the tropics and extratropics. *Science*, **275**, 805–807.
- Hazeleger, W., P. de Vries, and G. J. van Oldenborgh, 2001a: Do tropical cells ventilate the Indo-Pacific equatorial thermocline? *Geophys. Res. Lett.*, **28**, 1763–1766.
- , R. Seager, M. Visbeck, N. Naik, and K. Rodgers, 2001b: Impact of the midlatitude storm track on the upper Pacific Ocean. *J. Phys. Oceanogr.*, **31**, 616–636.
- , M. Visbeck, M. Cane, A. Karspeck, and N. Naik, 2001c: Decadal upper ocean variability in the tropical Pacific. *J. Geophys. Res.*, **106**, 8971–8988.
- , C. Severijns, R. Haarsma, F. Selten, and A. Sterl, 2003: SPEEDO—Model description and validation of a flexible coupled model for climate studies. KNMI Tech. Rep. 257, 38 pp.
- , R. Seager, M. Cane, and N. Naik, 2004: How can tropical Pacific Ocean heat transport vary? *J. Phys. Oceanogr.*, **34**, 320–333.
- Held, I. M., 2001: The partitioning of the poleward energy transport between the tropical ocean and atmosphere. *J. Atmos. Sci.*, **58**, 943–948.
- Kalnay, E., and Coauthors, 1996: The NCEP/NCAR 40-Year Reanalysis Project. *Bull. Amer. Meteor. Soc.*, **77**, 437–471.
- Kleeman, R., J. P. McCreary, and B. A. Klinger, 1999: A mechanism for generating ENSO decadal variability. *Geophys. Res. Lett.*, **26**, 1743–1746.
- Klinger, B. A., J. P. McCreary, and R. Kleeman, 2002: The relationship between oscillating subtropical wind stress and equatorial temperature. *J. Phys. Oceanogr.*, **32**, 1507–1521.
- Kushner, P. J., I. M. Held, and T. L. Delworth, 2001: Southern Hemisphere atmospheric circulation response to global warming. *J. Climate*, **14**, 2238–2249.
- Liu, J., X. Yuan, D. Rind, and D. G. Martinson, 2002: Mechanism study of the ENSO and southern high latitude climate teleconnections. *Geophys. Res. Lett.*, **29**, 1679, doi:10.1029/2002GL015143.
- Mantua, N. J., S. R. Hare, Y. Zhang, J. M. Wallace, and R. C. Francis, 1997: A Pacific interdecadal climate oscillation with impacts on salmon production. *Bull. Amer. Meteor. Soc.*, **78**, 1069–1079.
- Marshall, J., H. Johnson, and J. Goodman, 2001: A study of the interaction of the North Atlantic Oscillation with ocean circulation. *J. Climate*, **14**, 1399–1421.
- McCreary, J. P., and P. Lu, 1994: Interaction between the subtropical and tropical ocean. *J. Phys. Oceanogr.*, **24**, 1153–1165.
- McPhaden, M. J., and D. Zhang, 2002: Slowdown of the meridional overturning circulation in the upper Pacific Ocean. *Nature*, **415**, 603–608.
- Molteni, F., 2003: Atmospheric simulations using a GCM with simplified physical parameterizations. I: Model climatology and variability in multi-decadal experiments. *Climate Dyn.*, **20**, 175–191.
- Nonaka, M., S.-P. Xie, and J. P. McCreary, 2002: Decadal variations in the subtropical cells and equatorial Pacific SST. *Geophys. Res. Lett.*, **29**, 1116, doi:10.1029/2001GL013717.
- Peixoto, J. P., and A. H. Oort, 1992: *Physics of Climate*. American Institute of Physics, 520 pp.
- Schneider, N. S., S. Venzke, A. J. Miller, D. W. Pierce, T. O. Barnett, C. Deser, and M. Latif, 1999: Pacific thermocline bridge revisited. *Geophys. Res. Lett.*, **26**, 1329–1332.
- Seager, R., M. B. Blumenthal, and Y. Kushnir, 1995: An advective atmospheric mixed layer model for ocean modeling purposes: Global simulation of surface heat fluxes. *J. Climate*, **8**, 1951–1964.
- , N. Harnik, Y. Kushnir, W. Robinson, and J. Miller, 2003: Mechanisms of hemispherically symmetric climate variability. *J. Climate*, **16**, 2960–2978.
- Sun, D.-Z., 2000: The heat sources and sinks of the 1986–87 El Niño. *J. Climate*, **13**, 3533–3550.
- Sutton, R., and P.-P. Mathieu, 2002: Response of the atmosphere-ocean mixed-layer system to anomalous ocean heat-flux convergence. *Quart. J. Roy. Meteor. Soc.*, **128**, 1259–1275.
- Talley, L. D., 2003: Shallow, intermediate, and deep overturning components of the global heat budget. *J. Phys. Oceanogr.*, **33**, 530–560.

- Trenberth, K. E., and J. M. Caron, 2001: Estimates of meridional atmosphere and ocean heat transports. *J. Climate*, **14**, 3433–3443.
- , and D. P. Stepaniak, 2003: Covariability of components of poleward atmospheric energy transport on seasonal and interannual time scales. *J. Climate*, **16**, 3691–3705.
- , G. W. Branstator, D. Karoly, A. Kumar, N.-C. Lau, and C. Ropelewski, 1998: Progress during TOGA in understanding and modeling global teleconnections associated with tropical sea surface temperatures. *J. Geophys. Res.*, **103**, 14 291–14 324.
- Wielicki, B. A., and Coauthors, 2002: Evidence for large decadal variability in the tropical mean radiative energy budget. *Science*, **295**, 841–844.
- Winton, M., 2003: On the climatic impact of ocean circulation. *J. Climate*, **16**, 2875–2889.
- Zebiak, S. E., 1989: Oceanic heat content variability and El Niño cycles. *J. Phys. Oceanogr.*, **19**, 475–486.
- Zhang, Y., J. M. Wallace, and D. S. Battisti, 1997: ENSO-like interdecadal variability: 1900–1993. *J. Climate*, **10**, 1004–1020.
- Zhang, Y.-C., and W. B. Rossow, 1997: Estimating meridional energy transports by the atmospheric and oceanic general circulations using boundary fluxes. *J. Climate*, **10**, 2358–2373.